$VH(b\bar{b}/c\bar{c})$ analyses in ATLAS

COMETA workshop
20th – 21st February 2025
Vienna

Romain Bouquet

- **Probing the Yukawa (Y_q) couplings in the quark sector is a milestone of the LHC**
- Presentation focussing on the **ATLAS $VH(b\bar{b}/c\bar{c})$, $V \to$ leptons process**
  - **Most sensitive for Y_b and Y_c coupling measurements**
  - **$VH(b\bar{b}/c\bar{c})$ Legacy Run 2 analysis (Sept. 2024): arXiv:2410.19611** $\rightarrow$ submitted to JHEP
- **Disclaimer:** not covering here **the hadronic $VH(b\bar{b})$, $V \to qq$ analysis** (Phys. Rev. Lett. 132 (2024) 131802)

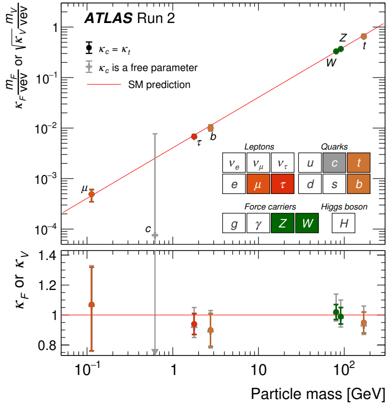

Higgs coupling to particles & VH mechanism

- Main decay of the Higgs: $\mathrm{BR}(H \to b\bar{b}) \approx 58\%$
- Other decay of interest: $\mathrm{BR}(H \to c\bar{c}) \approx 2.7\%$

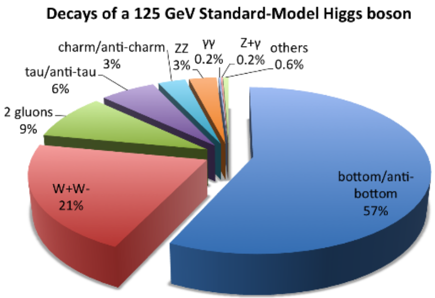

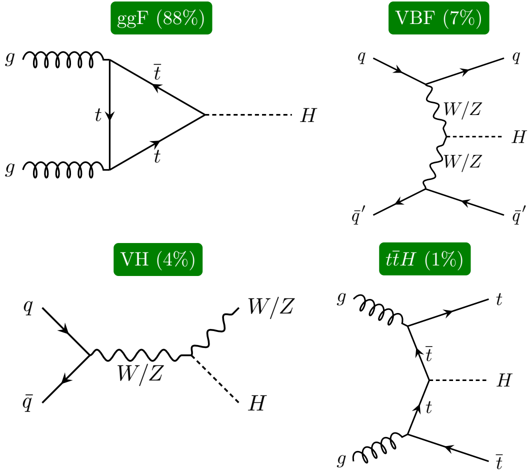

- Why the VH mechanism is of interest despite its low cross-section?
  - Strong reduction of QCD background thanks to the leptonic decay of the W/Z boson
  - Study both coupling of the Higgs with vector boson and coupling to b- & c-quarks
  - First observation of $H \to b\bar{b}$ thanks to the VH mechanism both for ATLAS and CMS in 2018

$VH(b\bar{b})$, 3 channels & 2 topologies: resolved & boosted

➢ **$VH, H \to b\bar{b}$ analysis: production of a Higgs boson with $pp \to VH, H \to b\bar{b}$ in 3 (charged)-lepton channels:**

- **0L channel**: $Z \to \nu\bar{\nu}$ $\Rightarrow$ 0 lepton in the state + large $E_{\mathrm{T}}^{\mathrm{miss}}$
- **1L channel**: $W \to \ell\nu$ $\Rightarrow$ 1 lepton in the final state + $E_{\mathrm{T}}^{\mathrm{miss}}$
- **2L channel**: $Z \to \ell^+\ell^-$ $\Rightarrow$ 2 leptons in the final state

0L channel

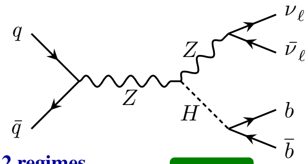

1L channel

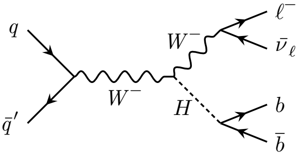

2L channel

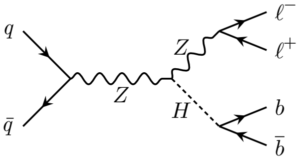

2 regimes

Resolved

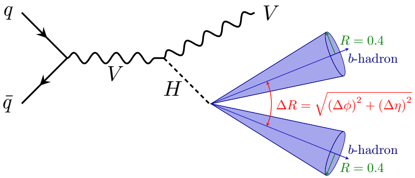

Boosted

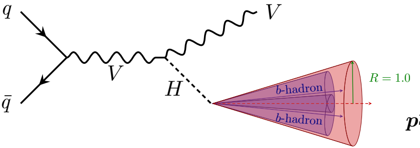

Angular distance between jets

$$\boldsymbol{\Delta R \approx \frac{2m_H}{p_{\mathrm{T}}^H}}$$

$$\boldsymbol{m_H = 125 \text{ GeV}}$$

$\Rightarrow$ boosted for $p_{\mathrm{T}}^H \approx$ few hundred of GeV

$VH(c\bar{c})$, 3 channels & only 1 topology: resolved

0L channel

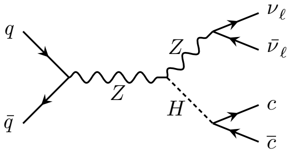

1L channel

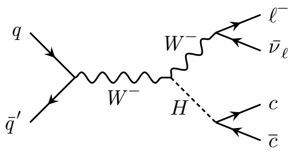

2L channel

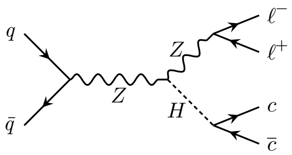

Resolved

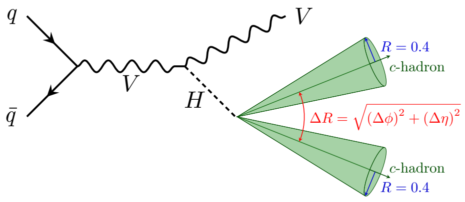

For the Run 2, no *c*-tagger for track-jets was provided by ATLAS

⇒ no reconstruction with the boosted topology

$Z+$jets

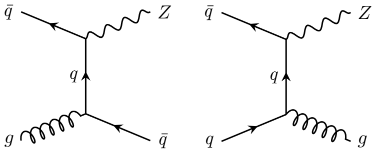

$W+$jets

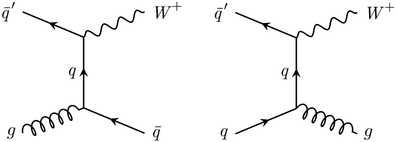

ttbar

lepton+jets

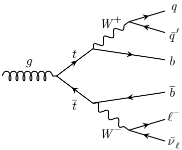

dilepton

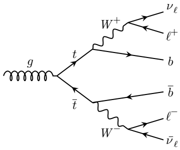

Single top

s-channel

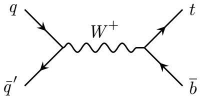

t-channel

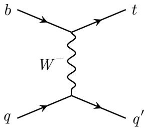

Wt

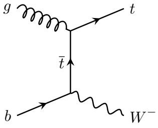

Diboson (VV)

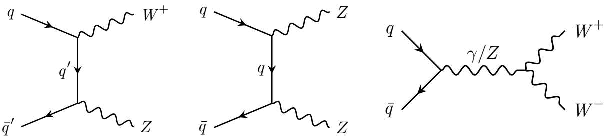

- Single top & diboson are subdominant backgrounds
- Residual multijet background reduced at percent level for 0L & 1L, negligible for 2L channel
- **Use machine learning algorithms to discriminate signal from background events**

$VH(b\bar{b}/c\bar{c})$ resolved topologies: division of phase space & Higgs candidate jets selection

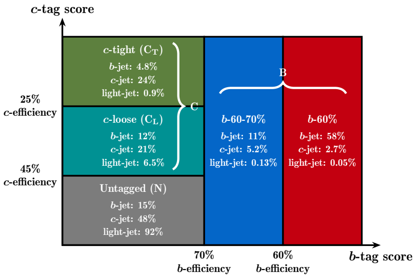

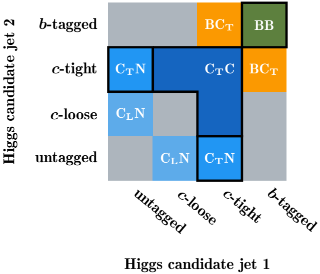

- **DL1r tagger, 2D-tagging scheme**: othogonal b- & c-tagging categories
  $\rightarrow$ **ensures orthogonality between the resolved $VH(b\bar{b})$ and $VH(c\bar{c})$ analyses**
- **Resolved VH, $H \rightarrow b\bar{b}$**: require exactly 2 b-tagged jets
  $\rightarrow$ BB pair = Higgs candidate
- **Resolved VH, $H \rightarrow c\bar{c}$**: require at least one tightly c-tagged (C_T) jet
  - ***2 different signal regions***: C_TC, C_TN
    $\rightarrow$ c-tagging efficiency is lower hence using the c-tight-untagged (C_TN) region
  - ***2 highest ranked jets = Higgs candidate***
    Ranking in 2 steps:
    - Order jets by tagging category: $C_T > C_L > N$
    - If several jets are in the same category order them by p_T

$VH(b\bar{b}/c\bar{c})$ resolved topologies: division of phase space & Higgs candidate jets selection

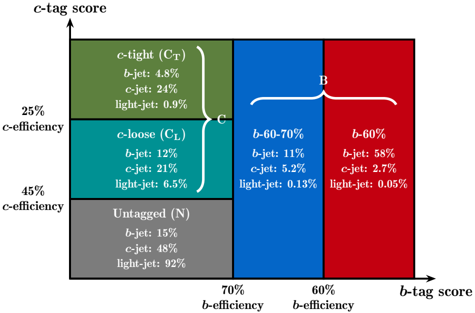

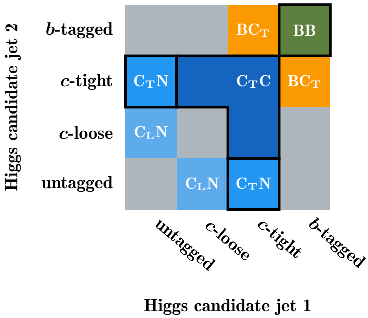

- Use the **2, 3-/$\geq$ 3-jets**, sometimes even the **4-/$\geq$ 4-jets** categories $\rightarrow$ cover possible initial (ISR) or final (FSR) state radiation(s) (see overview slide)
- **Some *b*-/*c*-vetos are applied to avoid overlap between $VH(b\bar{b})$ and $VH(c\bar{c})$** in the 3-/$\geq$ 3-jets & 4-/$\geq$ 4-jets categories
- **BC_T control region** to constrain the **Top(*bc*) background**, common to $VH(b\bar{b})$ & $VH(c\bar{c})$
- **C_LN control region** to constrain **V+light backgrounds** for $VH(c\bar{c})$

$VH(b\bar{b})$ boosted topology: tagging strategy & Higgs candidate jet selection

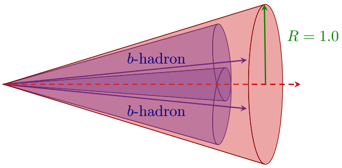

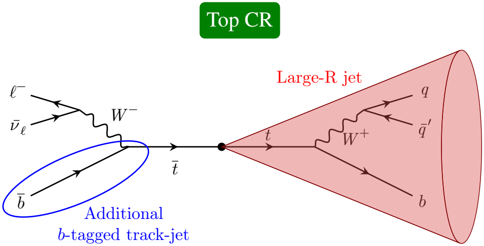

- Use the **DL1r 85% *b*-tagging efficiency WP on track-jet**
- **Leading large-R jet = Higgs candidate**
- **Require exactly 2 *b*-tagged track-jet out of the 3 leading track-jets**
- **Top CR** if at least one *b*-tagged track-jet is found outside of the leading large-R jet

Overview: signal (SR) & control (CR) regions

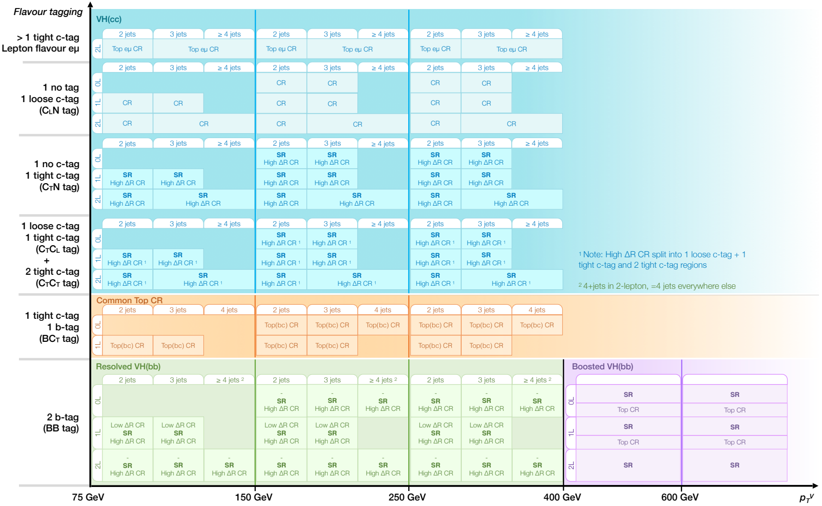

- ➢ **Complex analysis ≈60 SRs & ≈100 CRs** based on tagging & kinematic selections
- ➢ **$VH(b\bar{b})$ resolved topology for $p_T^V < 400$ GeV**
- ➢ **$VH(b\bar{b})$ boosted for $p_T^V > 400$ GeV**

An important cross-check: the diboson analyses $VZ, Z \to b\bar{b}$ and $VZ, Z \to c\bar{c}$ results

To ensure that the analysis is not biased
a $VZ, Z \to b\bar{b}/c\bar{c}$ measurement is performed with a simultaneous fit

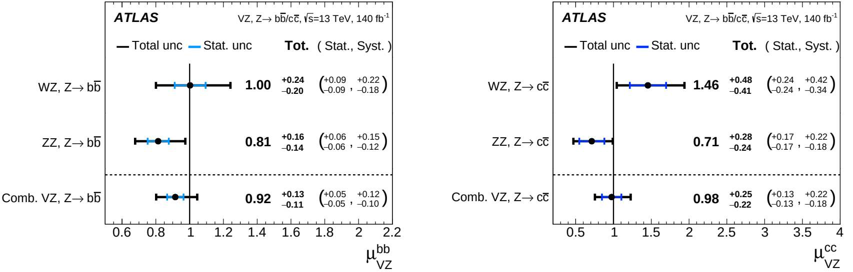

- **$VZ(b\bar{b})$ is observed with a significance greater than 10**
  - **$WZ(b\bar{b})$ obs. (exp.)**: 6.4σ (6.5σ) $\to$ **First observation**
  - **$ZZ(b\bar{b})$**: significance is greater than 10
- **$VZ(c\bar{c})$ obs. (exp.)**: 5.2σ (5.3σ) $\to$ **First ATLAS observation**
  - **$WZ(c\bar{c})$ obs. (exp.)**: 3.9σ (2.7σ)
  - **$ZZ(c\bar{c})$ obs. (exp.)**: 3.1σ (4.3σ)

NB: dedicated BDTs training to target the $VZ, Z \to b\bar{b}/c\bar{c}$ processes, but the kinematic selections and division of phase space is unchanged

$\Rightarrow$ **Results compatible with SM predictions**

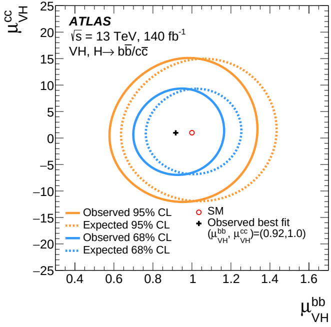

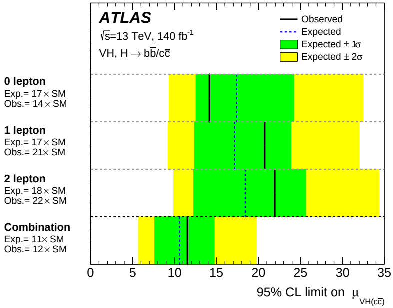

$$\mu_{VH}^{bb} = 0.92^{+0.16}_{-0.15} = 0.92 \pm 0.10\,(\text{stat.})^{+0.13}_{-0.11}\,(\text{syst.})$$
$$\mu_{VH}^{cc} = 1.0^{+5.4}_{-5.2} = 1.0^{+4.0}_{-3.9}\,(\text{stat.})^{+3.7}_{-3.5}\,(\text{syst.})$$

- **$VH(b\bar{b})$ obs. (exp.)**: 7.4σ (8.0σ) $\rightarrow$ **Most precise μ_{VH}^{bb} measurement: 15% precision, improved by 20% w.r.t. previous Run 2 analysis**
  - **$WH(b\bar{b})$ obs. (exp.)**: 5.3σ (5.5σ) $\rightarrow$ **First observation**
  - **$ZH(b\bar{b})$ obs. (exp.)**: 4.9σ (5.6σ)
- **$VH(c\bar{c})$ limit at 95% CL obs. (exp.)**: 11.5 (10.6) $\rightarrow$ **Strongest observed limit, factor 3 better than previous Run 2 analysis (obs. (exp.): 26 (31))**
- **Latest CMS results for comparison (also full Run 2)**:
  - **$VH(b\bar{b})$**: $\mu_{VH}^{bb} = 1.15^{+0.22}_{-0.20}$ $\rightarrow$ 20% precision on μ_{VH}^{bb} (Phys. Rev. D 109 (2024) 092011)
  - **$VH(c\bar{c})$ limit at 95% CL obs. (exp.)**: obs. (exp.): 14.4 (7.6) (Phys. Rev. Lett. 131 (2023) 061801)

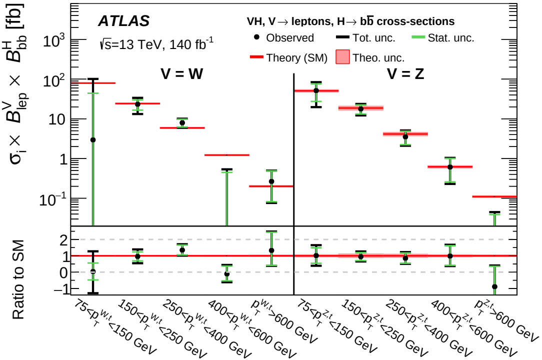

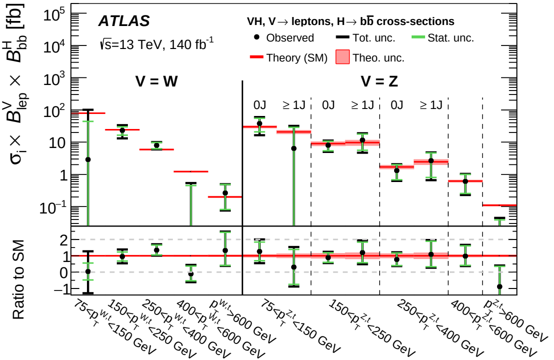

- **Extended STXS measurement** w.r.t. previous Run 2 analysis:
  - $75 < p_{\mathrm{T}}^{V} < 150$ GeV region added for WH
  - Split ZH into 0- and ≥ 1 additional jets for $p_{\mathrm{T}}^{V} < 400$ GeV
  - $p_{\mathrm{T}}^{V} > 600$ GeV region added (previously $p_{\mathrm{T}}^{V} > 400$ GeV)
- **Better *WH*-*ZH* decorrelation** w.r.t. previous round thanks to hadronic-τ treatment
- **Improvement of correlations by harmonizing reco & truth jet-p_{T} cuts**
- **STXS measurement allows for EFT interpretation, see Suman's talk**

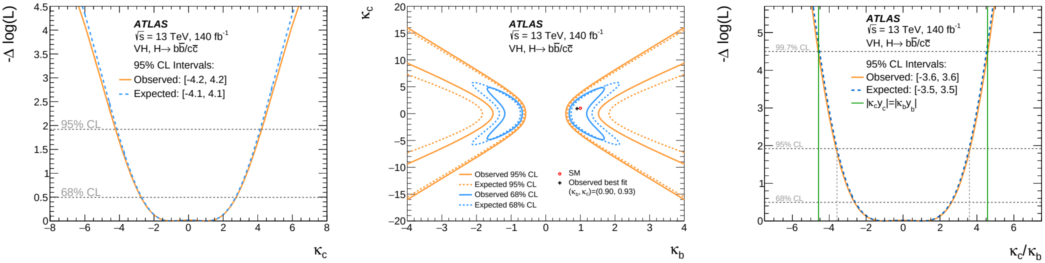

$$\mu^{bb}_{VH} = \frac{\kappa_b^2}{1 + B^{SM}_{Hbb}(\kappa_b^2 - 1) + B^{SM}_{Hcc}(\kappa_c^2 - 1)}, \quad \mu^{cc}_{VH} = \frac{\kappa_c^2}{1 + B^{SM}_{Hbb}(\kappa_b^2 - 1) + B^{SM}_{Hcc}(\kappa_c^2 - 1)} \Rightarrow \mu^{bb}_{VH} = \left(\frac{\kappa_b}{\kappa_c}\right)^2 \mu^{cc}_{VH}$$

➢ **1D scan:**
- Fixing $\kappa_b = 1$, obs. (exp.) 95% CL constraint: $\boldsymbol{|\kappa_c| < 4.2}$ **(**$\boldsymbol{|\kappa_c| < 4.1}$**)**
- Fixing $\kappa_c = 1$, obs. (exp.) 95% CL constraint: $\boldsymbol{0.67 < |\kappa_b| < 1.38}$ **(**$\boldsymbol{0.72 < |\kappa_b| < 1.56}$**)**

➢ **Exclusion of universality κ_c/κ_b with almost 3 sigma (right plot)**
i.e. Higgs-to-charm coupling is weaker than the Higgs-to-bottom coupling

Central role of flavour tagging for the $VH(b\bar{b}/c\bar{c})$ analysis

arXiv:2404.01071

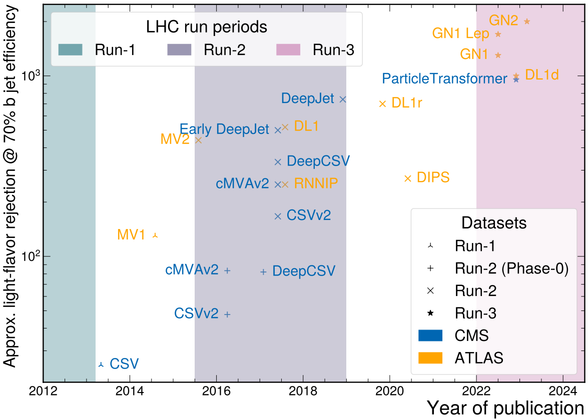

- **Reminder: observation of $H \to b\bar{b}$ in 2018 by ATLAS and CMS**
- **6 years later, precision measurement of the Higgs-to-bottom coupling**
- Every ≈ 2 years a new set of taggers is released by ATLAS and CMS since Run 1 with significant rejection improvements!

How about future flavour tagging improvements? Small-R jet GNN taggers!

FTAG-2023-01 & FTAG-2023-07

b-tagger rejection

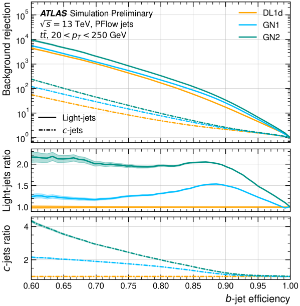

b-tagger rejection with SF

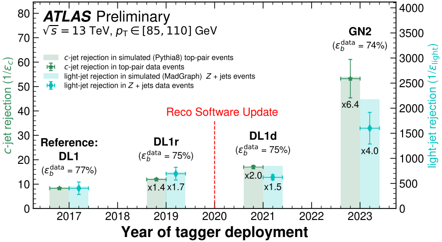

c-tagger rejection

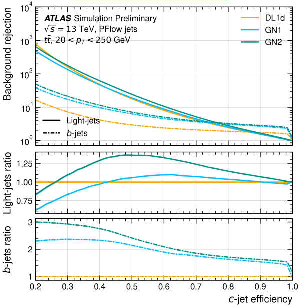

- ➢ **Still room for significant improvements with GNN transformer based algorithms**. More complex w.r.t. simple DNN (DL1r) algorithm + more low level information provided *e.g.* tracks, hits information. . .
- ➢ **Training taking into account calibration will be crucial in the future** to not washout performance increase!
- ➢ **See Lorenzo's talk about taggers exploiting timing information** (more distant future)

How about future flavour tagging improvements? Large-R jet GNN taggers!

ATL-PHYS-PUB-2023-021

Xbb-tagger rejection

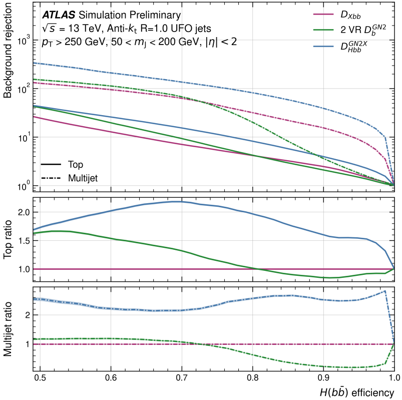

Xcc-tagger rejection

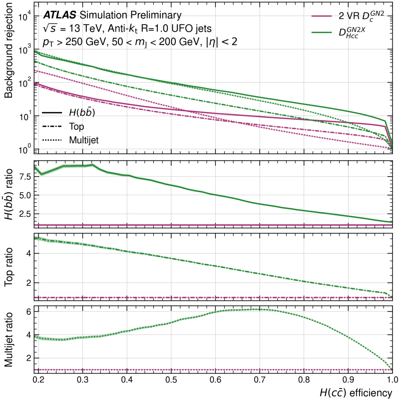

- **Change in philosophy**: tag large-R jet as potential $X \to b\bar{b}/c\bar{c}$ decay instead of track-jets within large-R jet $\to$ Take into account tracks correlations hence improving tagging performances
- **First $X \to c\bar{c}$ tagger within ATLAS** $\to$ Opens the door for a boosted $VH(c\bar{c})$ analysis!
- **See Jackson's talk for more info on Xbb/cc taggers**

- $VH(c\bar{c})$ **constraint improved between Run 2 & Legacy Run 2 analyses**, thanks to:
  - **Improved flavour tagging performances**: reduction of non c-jet background by $\approx$ 40% for the same signal efficiency $\rightarrow$ 25% gain in sensitivity
  - **Analysis refinements**: use of the BDT approach instead of dijet invariant mass $\rightarrow$ 40% gain in sensitivity
  - **Background sample statistic increase**: larger V+jets background samples simulation + use of truth tagging reweighting techniques (see backup)
- **Reaching the Legacy Run 2 sensitivity with the Run 2 analysis strategy would have required $\approx$ 9 times more data than collected at the Run 2 (see coming slide)**
  $\rightarrow$ **Impressive improvements while analyzing the exact same dataset!**
- **The Legacy Run 2 measurement is still largely statistically limited**
  $\rightarrow$ Gain of sensitivity by collecting more data. $3000\ \mathrm{fb}^{-1}$ expected for the HL-LHC

HL-LHC projection: towards the observation of the Higgs-to-charm coupling

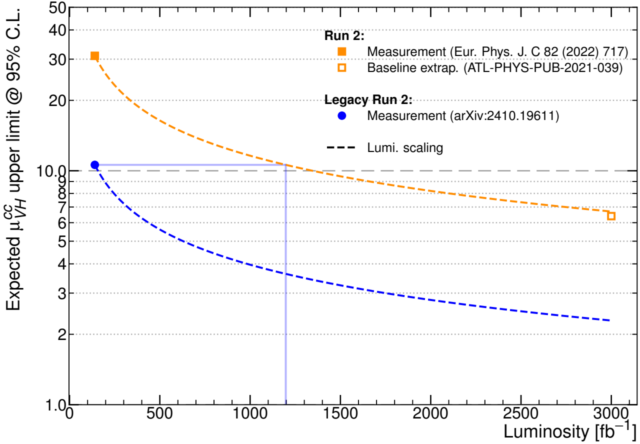

- **Expect reaching better sensitivity than presented here** thanks to GNN flavour tagging algorithms + analysis refinements
- Simple lumi scaling of Run 2 and Legacy Run 2 results assume all uncertainties scale as $\sqrt{L/L'}$ with $L = 140\ \text{fb}^{-1}$ = Run 2 lumi & L' = measurement lumi

- ➢ **$VH(b\bar{b})$ measurement has entered the precision era**:
  - Most precise measurement of Higgs-to-bottom coupling to date (15% precision on μ_{VH}^{bb})
  - Extended STXS measurement w.r.t. previous Run 2 analysis
- ➢ **$VH(c\bar{c})$ measurement**:
  - Best observed upper limit constraint: 12 times the SM predictions (factor 3 better than the previous Run 2 analysis)
  - Higgs-to-charm vs Higgs-to-bottom universality excluded (at almost 3 sigma)
- ➢ **Diboson analysis as cross-check**
  - Compatible with SM expectation
  - Observation of the $WZ(b\bar{b})$ process and first ATLAS observation of $VZ(c\bar{c})$
- ➢ **Main axes of improvements for the $VH(b\bar{b}/c\bar{c})$ Legacy Run 2 analysis were**:
  - Performance improvement in particular flavour tagging
  - Analysis refinements: extension of the BDT approach for boosted $VH(b\bar{b})$, and the $VH(c\bar{c})$ analyses, harmonization of CRs, MC sample size…
- ➢ **Future short or long terms improvements:**
  - Small-R jet and large-R jets GNN taggers
  - For the first time boosted $VH(c\bar{c})$ will be possible thanks to the GNN $X \to c\bar{c}$ tagger
  - Collected data will allow further constraining in particular the Higgs-to-charm coupling (can we reach it's observation at the end of HL-LHC?)

Backup

$VH(b\bar{b}/c\bar{c})$ resolved topologies: Low (CRLow) and High (CRHigh) ΔR control regions

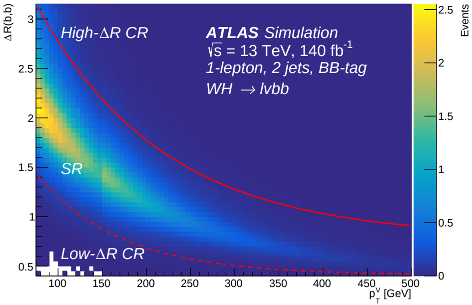

Contour defined as $f(p_{\mathrm{T}}^{V}) = a \times \exp\left(b + c \times p_{\mathrm{T}}^{V}\right)$

- **Low ΔR CR enriched in W+jets & $t\bar{t}$ backgrounds** (only used for VH, $H \to b\bar{b}$ 1L channel)
- **High ΔR CR enriched in $t\bar{t}$ & V+jets backgrounds**

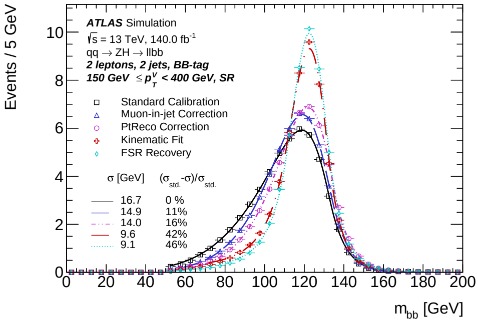
ATLAS Simulation
√s = 13 TeV, 140.0 fb-1
qq → ZH → llbb
2 leptons, 2 jets, BB-tag
150 GeV ≤ pTV < 400 GeV, SR
Standard Calibration
Muon-in-jet Correction
PtReco Correction
Kinematic Fit
FSR Recovery
σ [GeV] (σstd.-σ)/σstd.
16.7 0 %
14.9 11%
14.0 16%
9.6 42%
9.1 46%
Events / 5 GeV
mbb [GeV]

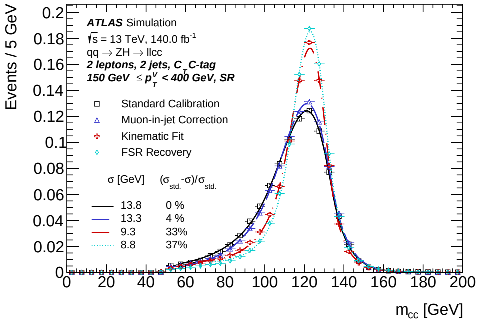
ATLAS Simulation
√s = 13 TeV, 140.0 fb-1
qq → ZH → llcc
2 leptons, 2 jets, CTC-tag
150 GeV ≤ pTV < 400 GeV, SR
Standard Calibration
Muon-in-jet Correction
Kinematic Fit
FSR Recovery
σ [GeV] (σstd.-σ)/σstd.
13.8 0 %
13.3 4 %
9.3 33%
8.8 37%
Events / 5 GeV
mcc [GeV]

Flavour tagging scale factors

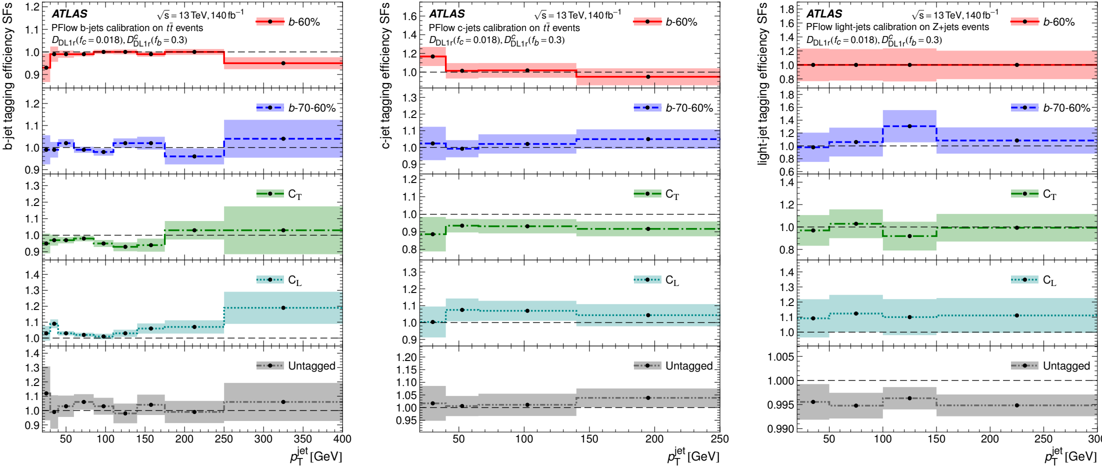

Truth tagging = reweighting of events based on their probability to pass tagging requirements

- Significant increase in statistics for simulated events especially for non-targeted flavour components for background processes
- Requires a precise knowledge of jet tagging efficiencies otherwise mismodelling introduced

Usual Truth Tagging: determination of jet tagging efficiency with (p_{T}, η) of jets

- Not ideal as correlations between jets are not considered
- Efficiency prediction only based on 2 variables

New GNN approach: consider kinematic properties of events and correlations between jets

- Simultaneous prediction of efficiencies for all jets in the event
- Large reduction of mismodelling

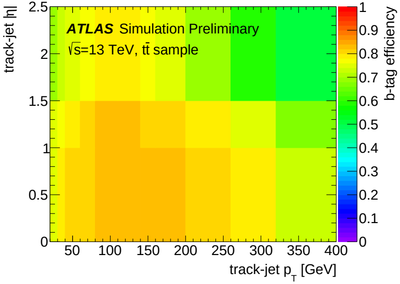

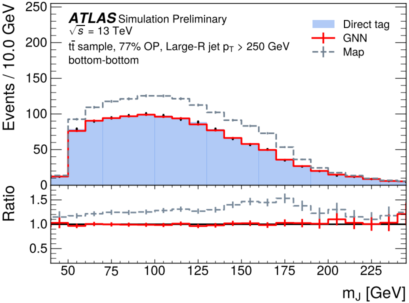

	Resolved VH, $H \to b\bar{b}, c\bar{c}$			Boosted VH, $H \to b\bar{b}$		
Variable	0-lepton	1-lepton	2-lepton	0-lepton	1-lepton	2-lepton
m_H	✓	✓	✓	✓	✓	✓
$m_{j_1 j_2 j_3}$	✓	✓	✓			
$p_T^{j_1}$	✓	✓	✓	✓	✓	✓
$p_T^{j_2}$	✓	✓	✓	✓	✓	✓
$p_T^{j_3}$				✓	✓	✓
$\sum p_T^{j_i}, i > 2$	✓	✓	✓			
$\text{bin}_{D_{\text{DL1r}}}(j_1)$	✓	✓	✓	✓	✓	✓
$\text{bin}_{D_{\text{DL1r}}}(j_2)$	✓	✓	✓	✓	✓	✓
p_T^V	$\equiv E_T^{\text{miss}}$	✓	✓	$\equiv E_T^{\text{miss}}$	✓	✓
E_T^{miss}	✓	✓		✓	✓	
$E_T^{\text{miss}}/\sqrt{S_T}$			✓			
$\lvert\Delta\phi(\boldsymbol{V}, \boldsymbol{H})\rvert$	✓	✓	✓	✓	✓	✓
$\lvert\Delta y(\boldsymbol{V}, \boldsymbol{H})\rvert$		✓	✓		✓	✓
$\Delta R(\boldsymbol{j_1}, \boldsymbol{j_2})$	✓	✓	✓	✓	✓	✓
$\min[\Delta R(\boldsymbol{j_i}, \boldsymbol{j_1} \text{ or } \boldsymbol{j_2})], i > 2$	✓	✓				
N(track-jets in J)				✓	✓	✓
N(add. small-R jets)				✓	✓	✓
colour ring				✓	✓	✓
$\lvert\Delta\eta(\boldsymbol{j_1}, \boldsymbol{j_2})\rvert$	✓					
$H_T + E_T^{\text{miss}}$	✓					
m_T^W		✓				
m_{top}		✓				
$\min[\Delta\phi(\boldsymbol{\ell}, \boldsymbol{j_1} \text{ or } \boldsymbol{j_2})]$		✓				
p_T^{ℓ}					✓	
$(p_T^{\ell} - E_T^{\text{miss}})/p_T^V$					✓	
$m_{\ell\ell}$			✓			
$\cos\theta^*(\boldsymbol{\ell^-}, \boldsymbol{V})$			✓			✓

Relative background composition for the $VH(b\bar{b}/c\bar{c})$ resolved topology

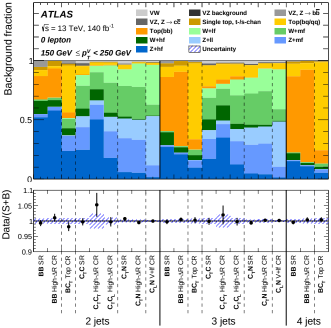

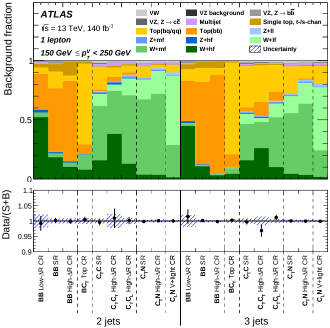

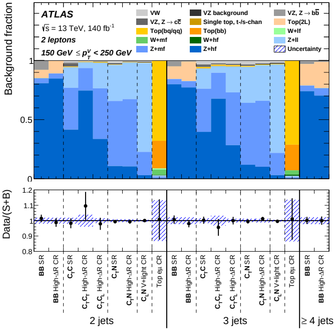

Relative background composition for the $VH(b\bar{b})$ boosted topology

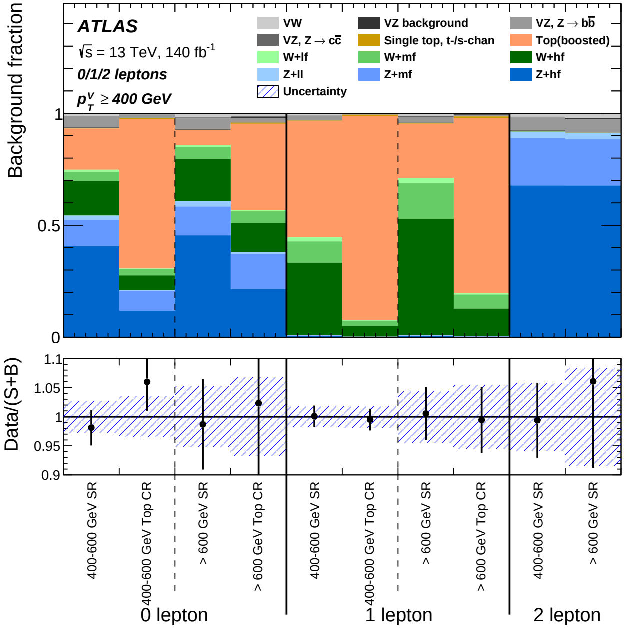

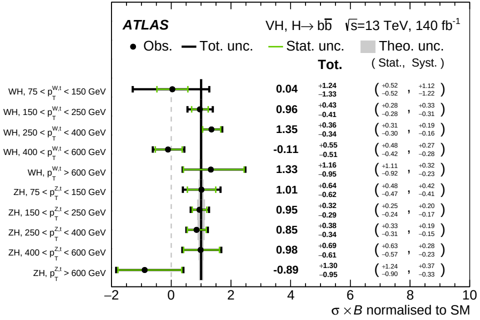
ATLAS
VH, H→ bb̄ √s=13 TeV, 140 fb-1
Obs. Tot. unc. Stat. unc. Theo. unc.
Tot. (Stat., Syst.)
WH, 75 < pTW,t < 150 GeV 0.04 +1.24 −1.33 (+0.52 −0.52 , +1.12 −1.22)
WH, 150 < pTW,t < 250 GeV 0.96 +0.43 −0.41 (+0.28 −0.28 , +0.33 −0.31)
WH, 250 < pTW,t < 400 GeV 1.35 +0.36 −0.34 (+0.31 −0.30 , +0.19 −0.16)
WH, 400 < pTW,t < 600 GeV -0.11 +0.55 −0.51 (+0.48 −0.42 , +0.27 −0.28)
WH, pTW,t > 600 GeV 1.33 +1.16 −0.95 (+1.11 −0.92 , +0.32 −0.23)
ZH, 75 < pTZ,t < 150 GeV 1.01 +0.64 −0.62 (+0.48 −0.47 , +0.42 −0.41)
ZH, 150 < pTZ,t < 250 GeV 0.95 +0.32 −0.29 (+0.25 −0.24 , +0.20 −0.17)
ZH, 250 < pTZ,t < 400 GeV 0.85 +0.38 −0.34 (+0.33 −0.31 , +0.19 −0.15)
ZH, 400 < pTZ,t < 600 GeV 0.98 +0.69 −0.61 (+0.63 −0.57 , +0.28 −0.23)
ZH, pTZ,t > 600 GeV -0.89 +1.30 −0.95 (+1.24 −0.90 , +0.37 −0.33)
−2 0 2 4 6 8 10
σ × B normalised to SM

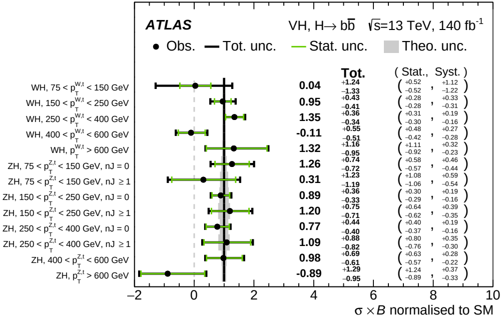
ATLAS
VH, H→ bb̄ √s=13 TeV, 140 fb-1
Obs. Tot. unc. Stat. unc. Theo. unc.
Tot. (Stat., Syst.)
WH, 75 < pTW,t < 150 GeV 0.04 +1.24 −1.33 (+0.52 −0.52 , +1.12 −1.22)
WH, 150 < pTW,t < 250 GeV 0.95 +0.43 −0.41 (+0.28 −0.28 , +0.33 −0.31)
WH, 250 < pTW,t < 400 GeV 1.35 +0.36 −0.34 (+0.31 −0.30 , +0.19 −0.16)
WH, 400 < pTW,t < 600 GeV -0.11 +0.55 −0.51 (+0.48 −0.42 , +0.27 −0.28)
WH, pTW,t > 600 GeV 1.32 +1.16 −0.95 (+1.11 −0.92 , +0.32 −0.23)
ZH, 75 < pTZ,t < 150 GeV, nJ = 0 1.26 +0.74 −0.72 (+0.58 −0.57 , +0.46 −0.44)
ZH, 75 < pTZ,t < 150 GeV, nJ ≥ 1 0.31 +1.23 −1.19 (+1.08 −1.06 , +0.59 −0.54)
ZH, 150 < pTZ,t < 250 GeV, nJ = 0 0.89 +0.36 −0.33 (+0.30 −0.29 , +0.19 −0.16)
ZH, 150 < pTZ,t < 250 GeV, nJ ≥ 1 1.20 +0.75 −0.71 (+0.64 −0.62 , +0.39 −0.35)
ZH, 250 < pTZ,t < 400 GeV, nJ = 0 0.77 +0.44 −0.40 (+0.40 −0.37 , +0.19 −0.16)
ZH, 250 < pTZ,t < 400 GeV, nJ ≥ 1 1.09 +0.88 −0.82 (+0.80 −0.76 , +0.35 −0.30)
ZH, 400 < pTZ,t < 600 GeV 0.98 +0.69 −0.61 (+0.63 −0.57 , +0.28 −0.22)
ZH, pTZ,t > 600 GeV -0.89 +1.29 −0.95 (+1.24 −0.89 , +0.37 −0.33)
−2 0 2 4 6 8 10
σ × B normalised to SM

Migration matrix

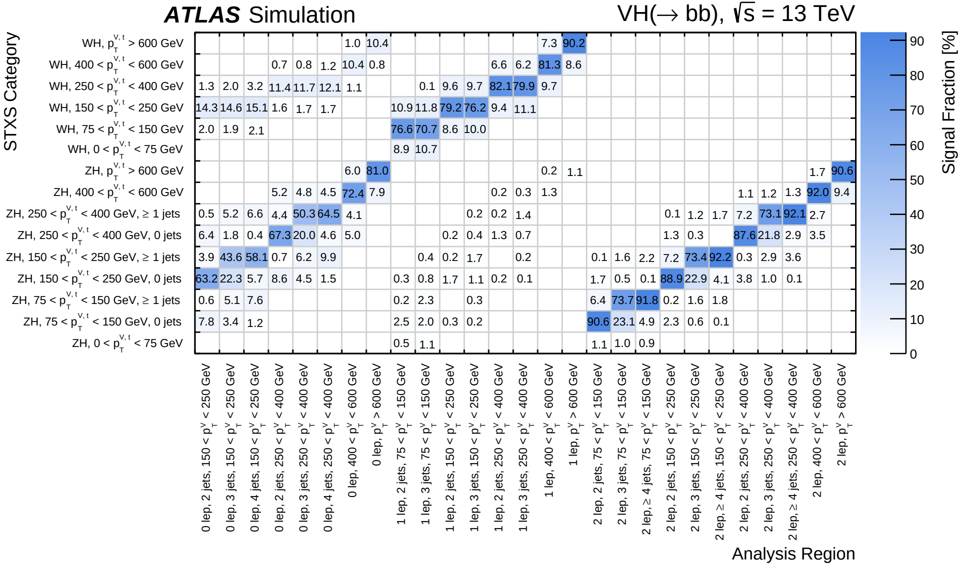

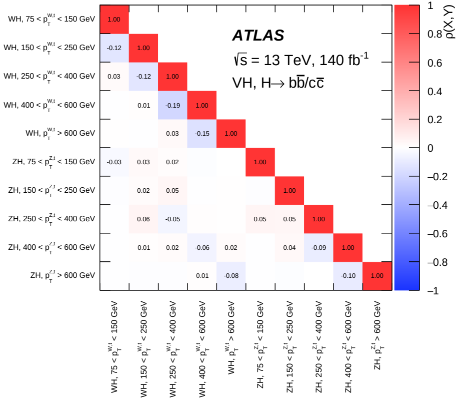
ATLAS
√s = 13 TeV, 140 fb-1
VH, H→ bb̄/cc̄
ρ(X,Y)

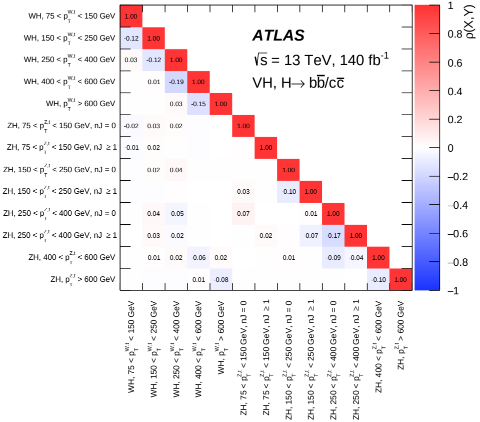
ATLAS
√s = 13 TeV, 140 fb-1
VH, H→ bb̄/cc̄
ρ(X,Y)

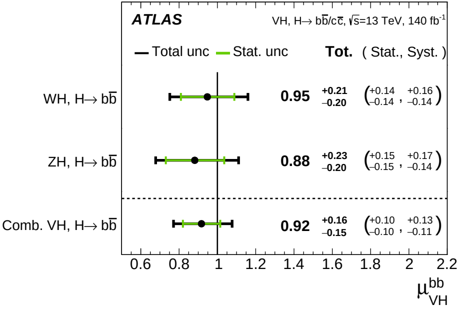

ATLAS
VH, H→ bb̄/cc̄, √s=13 TeV, 140 fb-1
Total unc
Stat. unc
Tot. (Stat., Syst.)
WH, H→ bb̄
0.95 +0.21 −0.20 (+0.14 −0.14 , +0.16 −0.14)
ZH, H→ bb̄
0.88 +0.23 −0.20 (+0.15 −0.15 , +0.17 −0.14)
Comb. VH, H→ bb̄
0.92 +0.16 −0.15 (+0.10 −0.10 , +0.13 −0.11)
μ bb VH

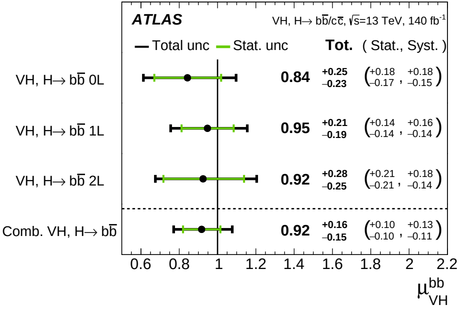

ATLAS
VH, H→ bb̄/cc̄, √s=13 TeV, 140 fb-1
Total unc
Stat. unc
Tot. (Stat., Syst.)
VH, H→ bb̄ 0L
0.84 +0.25 −0.23 (+0.18 −0.17 , +0.18 −0.15)
VH, H→ bb̄ 1L
0.95 +0.21 −0.19 (+0.14 −0.14 , +0.16 −0.14)
VH, H→ bb̄ 2L
0.92 +0.28 −0.25 (+0.21 −0.21 , +0.18 −0.14)
Comb. VH, H→ bb̄
0.92 +0.16 −0.15 (+0.10 −0.10 , +0.13 −0.11)
μ bb VH

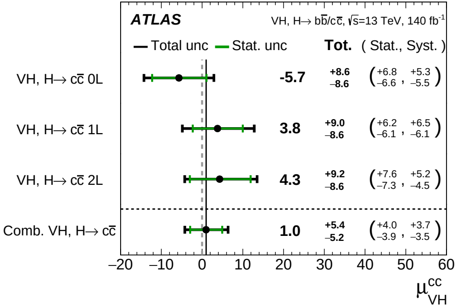

ATLAS
VH, H→ bb̄/cc̄, √s=13 TeV, 140 fb-1
Total unc
Stat. unc
Tot. (Stat., Syst.)
VH, H→ cc̄ 0L
-5.7 +8.6 −8.6 (+6.8 −6.6 , +5.3 −5.5)
VH, H→ cc̄ 1L
3.8 +9.0 −8.6 (+6.2 −6.1 , +6.5 −6.1)
VH, H→ cc̄ 2L
4.3 +9.2 −8.6 (+7.6 −7.3 , +5.2 −4.5)
Comb. VH, H→ cc̄
1.0 +5.4 −5.2 (+4.0 −3.9 , +3.7 −3.5)
μ cc VH

Source of uncertainty		σ_μ			
		$VH,\ H \to b\bar{b}$	$WH,\ H \to b\bar{b}$	$ZH,\ H \to b\bar{b}$	$VH,\ H \to c\bar{c}$
Total		0.153	0.204	0.216	5.31
Statistical		0.097	0.139	0.153	3.94
Systematic		0.118	0.149	0.153	3.57
Statistical uncertainties					
Data statistical		0.090	0.129	0.139	3.67
$t\bar{t}$ $e\mu$ control region		0.009	0.014	0.027	0.08
Background floating normalisations		0.034	0.049	0.042	1.24
Other VH floating normalisation		0.007	0.018	0.014	0.33
Simulation samples size		0.023	0.033	0.030	1.62
Experimental uncertainties					
Jets		0.027	0.035	0.030	1.02
$E_{\mathrm{T}}^{\mathrm{miss}}$		0.010	0.005	0.021	0.23
Leptons		0.003	0.002	0.010	0.25
b-tagging	b-jets	0.020	0.018	0.026	0.29
	c-jets	0.013	0.017	0.012	0.73
	light-flavour jets	0.005	0.008	0.008	0.66
Pile-up		0.008	0.017	0.002	0.23
Luminosity		0.006	0.007	0.006	0.08
Theoretical and modelling uncertainties					
Signal		0.076	0.074	0.101	0.72
Z + jets		0.042	0.018	0.081	1.77
W + jets		0.054	0.087	0.026	1.42
$t\bar{t}$ and Wt		0.018	0.033	0.018	1.02
Single top-quark (s-, t-ch.)		0.010	0.018	0.002	0.16
Diboson		0.033	0.039	0.049	0.52
Multijet		0.005	0.010	0.005	0.55

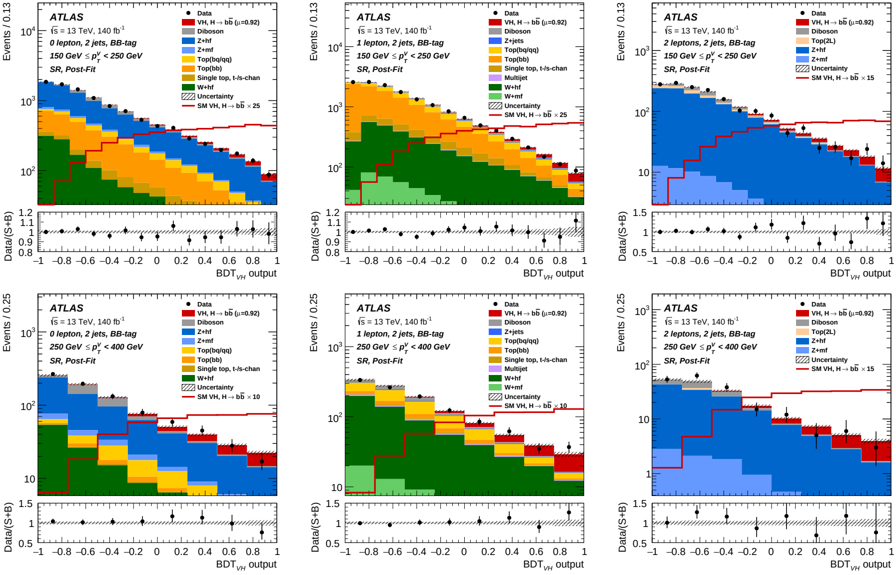
ATLAS
√s = 13 TeV, 140 fb⁻¹
0 lepton, 2 jets, BB-tag
150 GeV ≤ p_T^V < 250 GeV
SR, Post-Fit
Data
VH, H → bb̄ (μ=0.92)
Diboson
Z+hf
Z+mf
Top(bq/qq)
Top(bb)
Single top, t-/s-chan
W+hf
Uncertainty
SM VH, H → bb̄ × 25
Events / 0.13
Data/(S+B)
BDT_VH output
ATLAS
√s = 13 TeV, 140 fb⁻¹
1 lepton, 2 jets, BB-tag
150 GeV ≤ p_T^V < 250 GeV
SR, Post-Fit
Data
VH, H → bb̄ (μ=0.92)
Diboson
Z+jets
Top(bq/qq)
Top(bb)
Single top, t-/s-chan
Multijet
W+hf
W+mf
Uncertainty
SM VH, H → bb̄ × 25
Events / 0.13
Data/(S+B)
BDT_VH output
ATLAS
√s = 13 TeV, 140 fb⁻¹
2 leptons, 2 jets, BB-tag
150 GeV ≤ p_T^V < 250 GeV
SR, Post-Fit
Data
VH, H → bb̄ (μ=0.92)
Diboson
Top(2L)
Z+hf
Z+mf
Uncertainty
SM VH, H → bb̄ × 15
Events / 0.13
Data/(S+B)
BDT_VH output
ATLAS
√s = 13 TeV, 140 fb⁻¹
0 lepton, 2 jets, BB-tag
250 GeV ≤ p_T^V < 400 GeV
SR, Post-Fit
Data
VH, H → bb̄ (μ=0.92)
Diboson
Z+hf
Z+mf
Top(bq/qq)
Top(bb)
Single top, t-/s-chan
W+hf
Uncertainty
SM VH, H → bb̄ × 10
Events / 0.25
Data/(S+B)
BDT_VH output
ATLAS
√s = 13 TeV, 140 fb⁻¹
1 lepton, 2 jets, BB-tag
250 GeV ≤ p_T^V < 400 GeV
SR, Post-Fit
Data
VH, H → bb̄ (μ=0.92)
Diboson
Z+jets
Top(bq/qq)
Top(bb)
Single top, t-/s-chan
Multijet
W+hf
W+mf
Uncertainty
SM VH, H → bb̄ × 10
Events / 0.25
Data/(S+B)
BDT_VH output
ATLAS
√s = 13 TeV, 140 fb⁻¹
2 leptons, 2 jets, BB-tag
250 GeV ≤ p_T^V < 400 GeV
SR, Post-Fit
Data
VH, H → bb̄ (μ=0.92)
Diboson
Top(2L)
Z+hf
Z+mf
Uncertainty
SM VH, H → bb̄ × 15
Events / 0.25
Data/(S+B)
BDT_VH output

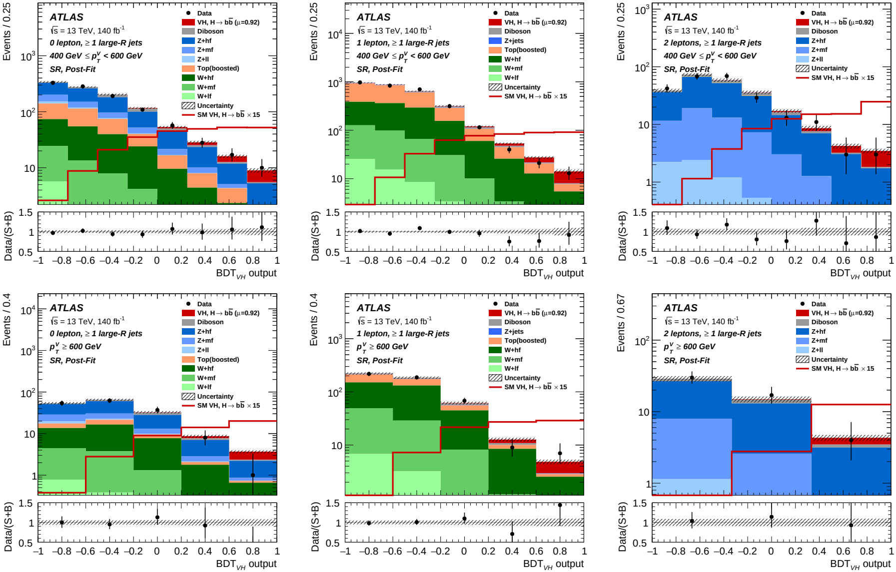

ATLAS
√s = 13 TeV, 140 fb⁻¹
0 lepton, ≥ 1 large-R jets
400 GeV ≤ p_T^V < 600 GeV
SR, Post-Fit
1 lepton, ≥ 1 large-R jets
2 leptons, ≥ 1 large-R jets
p_T^V ≥ 600 GeV
Data
VH, H → bb̄ (μ=0.92)
Diboson
Z+hf
Z+mf
Z+ll
Z+jets
Top(boosted)
W+hf
W+mf
W+lf
Uncertainty
SM VH, H → bb̄ × 15
Events / 0.25
Events / 0.4
Events / 0.67
Data/(S+B)
BDT$_{VH}$ output

Some $VH(c\bar{c})$ post-fit distributions

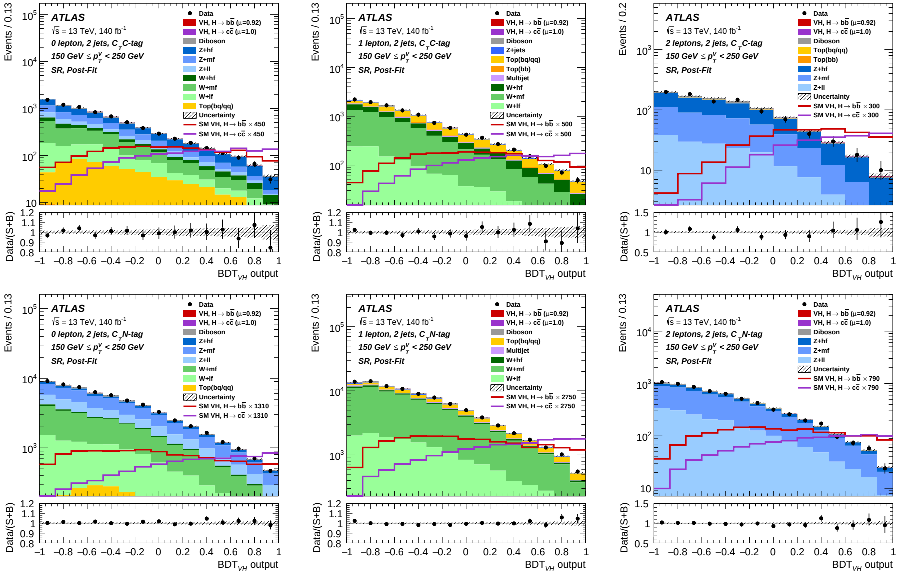

Eur. Phys. J. C 83 (2023) 681 & ATL-PHYS-PUB-2022-02

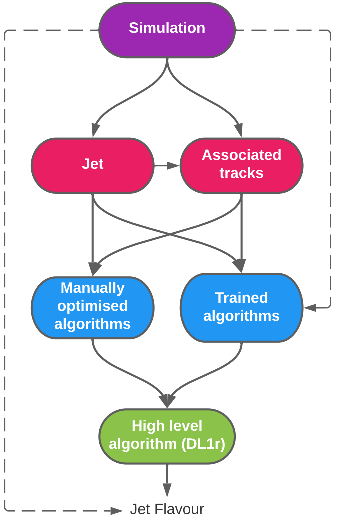

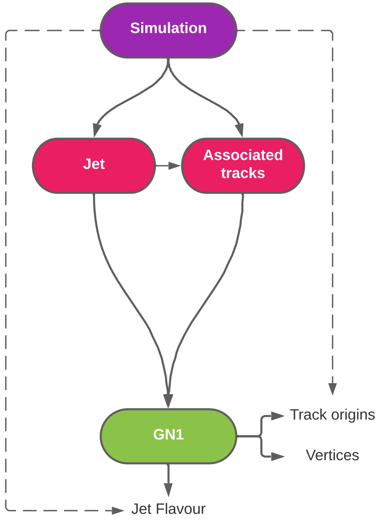

Eur. Phys. J. C 83 (2023) 681 & ATL-PHYS-PUB-2022-02

DL1r input variables

Input	Variable	Description	SVKine	JFKine	DL1	DL1r
Kinematics	p_T	Jet p_T	✓	✓	✓	✓
	η	Jet $\|\eta\|$	✓	✓	✓	✓
IP2D, IP3D	$\log(P_b/P_{light})$	Likelihood ratio of the b-jet to light-flavour jet hypotheses			✓	✓
	$\log(P_b/P_c)$	Likelihood ratio of the b-jet to c-jet hypotheses			✓	✓
	$\log(P_c/P_{light})$	Likelihood ratio of the c-jet to light-flavour jet hypotheses			✓	✓
RNNIP	P_b	b-jet probability				✓
	P_c	c-jet probability				✓
	P_{light}	light-flavour jet probability				✓
SV1	$m(SV)$	Invariant mass of tracks at the secondary vertex assuming pion mass	✓		✓	✓
	$f_E(SV)$	Jet energy fraction of the tracks associated with the secondary vertex	✓		✓	✓
	$N_{TrkAtVtx}(SV)$	Number of tracks used in the secondary vertex	✓		✓	✓
	$N_{2TrkVtx}(SV)$	Number of two-track vertex candidates	✓		✓	✓
	$L_{xy}(SV)$	Transverse distance between the primary and secondary vertices	✓		✓	✓
	$L_{xyz}(SV)$	Distance between the primary and secondary vertices	✓		✓	✓
	$S_{xyz}(SV)$	Distance between the primary and secondary vertices divided by its uncertainty	✓		✓	✓
	$\Delta R(\vec{p}_{jet}, \vec{p}_{vtx})(SV)$	ΔR between the jet axis and the direction of the secondary vertex relative to the primary vertex.	✓		✓	✓
JetFitter	$m(JF)$	Invariant mass of tracks from displaced vertices		✓	✓	✓
	$f_E(JF)$	Jet energy fraction of the tracks associated with the displaced vertices		✓	✓	✓
	$\Delta R(\vec{p}_{jet}, \vec{p}_{vtx})(JF)$	ΔR between the jet axis and the vectorial sum of momenta of all tracks attached to displaced vertices		✓	✓	✓
	$S_{xyz}(JF)$	Significance of the average distance between PV and displaced vertices		✓	✓	✓
	$N_{TrkAtVtx}(JF)$	Number of tracks from multi-prong displaced vertices		✓	✓	✓
	$N_{2TrkVtx}(JF)$	Number of two-track vertex candidates (prior to decay chain fit)		✓	✓	✓
	$N_{1\text{-trk vertices}}(JF)$	Number of single-prong displaced vertices		✓	✓	✓
	$N_{\geq 2\text{-trk vertices}}(JF)$	Number of multi-prong displaced vertices		✓	✓	✓
	$L_{xyz}(2^{nd})(JF)$	Distance of 2^{nd} vertex from PV		✓	✓	✓
	$L_{xy}(2^{nd})(JF)$	Transverse displacement of the 2^{nd} vertex		✓	✓	✓
	$m_{Trk}(2^{nd})(JF)$	Invariant mass of tracks associated with the 2^{nd} vertex		✓	✓	✓
	$E(2^{nd})(JF)$	Energy of the tracks associated with the 2^{nd} vertex		✓	✓	✓
	$f_E(2^{nd})(JF)$	Jet energy fraction of the tracks associated with the 2^{nd} vertex		✓	✓	✓
	$N_{TrkAtVtx}(2^{nd})(JF)$	Number of tracks associated with the 2^{nd} vertex		✓	✓	✓
	$\eta_{trk}^{min,max,avg}(2^{nd})(JF)$	Min., max. and avg. pseudorapidity of tracks at the 2^{nd} vertex		✓	✓	✓

Eur. Phys. J. C 83 (2023) 681 & ATL-PHYS-PUB-2022-02

GN1 input variables

Jet Input	Description
p_T	Jet transverse momentum
η	Signed jet pseudorapidity

Track Input	Description
q/p	Track charge divided by momentum (measure of curvature)
$d\eta$	Pseudorapidity of the track, relative to the jet η
$d\phi$	Azimuthal angle of the track, relative to the jet ϕ
d_0	Closest distance from the track to the PV in the longitudinal plane
$z_0 \sin\theta$	Closest distance from the track to the PV in the transverse plane
$\sigma(q/p)$	Uncertainty on q/p
$\sigma(\theta)$	Uncertainty on track polar angle θ
$\sigma(\phi)$	Uncertainty on track azimuthal angle ϕ
$s(d_0)$	Lifetime signed transverse IP significance
$s(z_0)$	Lifetime signed longitudinal IP significance
nPixHits	Number of pixel hits
nSCTHits	Number of SCT hits
nIBLHits	Number of IBL hits
nBLHits	Number of B-layer hits
nIBLShared	Number of shared IBL hits
nIBLSplit	Number of split IBL hits
nPixShared	Number of shared pixel hits
nPixSplit	Number of split pixel hits
nSCTShared	Number of shared SCT hits
nPixHoles	Number of pixel holes
nSCTHoles	Number of SCT holes
leptonID	Indicates if track was used in the reconstruction of an electron or muon (only for GN1 Lep)

GN2 Xbb/cc taggers input variables

ATL-PHYS-PUB-2023-021

Jet Input	**Description**
p_{T}	Large-R jet transverse momentum
η	Signed large-R jet pseudorapidity
mass	Large-R jet mass
Track Input	**Description**
q/p	Track charge divided by momentum (measure of curvature)
dη	Pseudorapidity of track relative to the large-R jet η
dϕ	Azimuthal angle of the track, relative to the large-R jet ϕ
d_0	Closest distance from track to primary vertex (PV) in the transverse plane
$z_0 \sin\theta$	Closest distance from track to PV in the longitudinal plane
$\sigma(q/p)$	Uncertainty on q/p
$\sigma(\theta)$	Uncertainty on track polar angle θ
$\sigma(\phi)$	Uncertainty on track azimuthal angle ϕ
$s(d_0)$	Lifetime signed transverse IP significance
$s(z_0 \sin\theta)$	Lifetime signed longitudinal IP significance
nPixHits	Number of pixel hits
nSCTHits	Number of SCT hits
nIBLHits	Number of IBL hits
nBLHits	Number of B-layer hits
nIBLShared	Number of shared IBL hits
nIBLSplit	Number of split IBL hits
nPixShared	Number of shared pixel hits
nPixSplit	Number of split pixel hits
nSCTShared	Number of shared SCT hits
subjetIndex	Integer label of which subjet track is associated to (GN2X + Subjets only)
Subjet Input	**Description** (Used only in GN2X + Subjets)
p_{T}	Subjet transverse momentum
η	Subjet signed pseudorapidity
mass	Subjet mass
energy	Subjet energy
dη	Pseudorapidity of subjet relative to the large-R jet η
dϕ	Azimuthal angle of subjet relative to the large-R jet ϕ
GN2 p_b	b-jet probability of subjet tagged using GN2
GN2 p_c	c-jet probability of subjet tagged using GN2
GN2 p_u	light flavour jet probability of subjet tagged using GN2
Flow Input	**Description** (Used only in GN2X + Flow)
p_{T}	Transverse momentum of flow constituent
energy	Energy of flow constituent
dη	Pseudorapidity of flow constituent relative to the large-R jet η
dϕ	Azimuthal angle of flow constituent relative to the large-R jet ϕ

The Standard Model & the Higgs boson

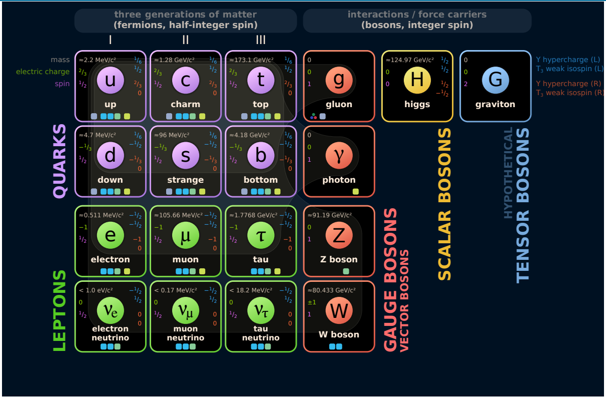

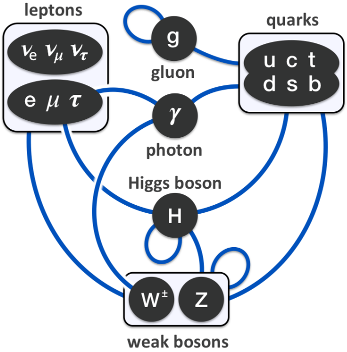

SM = Theory based on a Lagrangian formalism
that describes 3 out of 4 fundamental forces & properties of fermions & bosons

- **Strong interaction**: gluons (g) $\rightarrow$ *e.g.* confinement of quarks inside hadrons
- **Electromagnetic interaction**: photon (γ) $\rightarrow$ *e.g.* interaction between charged particles
- **Weak interaction**: $W^{\pm}$ & Z bosons $\rightarrow$ *e.g.* flavour violation, radioactivity

- **Fermions (half-integer spins, 3 families)**: leptons & quarks
- **Bosons (integer spins)**: g, γ, $W^{\pm}$, Z & H

$$\mathcal{L}_{SM} = \mathcal{L}_{EW} + \mathcal{L}_{QCD} + \underbrace{\mathcal{L}_{Higgs} + \mathcal{L}_{Yukawa}}_{\text{Higgs mechanism terms}}$$

Why are $\mathcal{L}_{Higgs} + \mathcal{L}_{Yukawa}$ terms needed?

- **The EW theory predicts a symmetry between the electromagnetic and weak forces, & massless particles…**
  But experimentally the 2 interactions are much different, & particles have masses
- **Brout-Englert-Higgs (BEH) mechanism**:

$$\mathcal{L}_{Higgs} = (D^{\mu}\phi)^{\dagger}(D_{\mu}\phi) - V(\phi) \quad (\phi = \text{2D complex scalar field})$$

$$V(\phi) = \mu^2 |\phi|^2 + \lambda |\phi|^4 \quad (V(\phi) = \text{Higgs potential})$$

- Spontaneous symmetry breaking for $\mu^2 < 0$ & $\lambda > 0$

$\mu^2 \geq 0$

$\phi_{min} = 0$

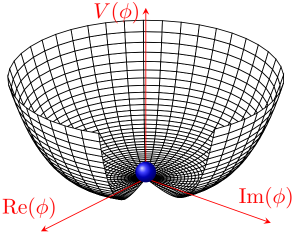

$\mu^2 < 0$

$|\phi_{min}|^2 = -\frac{\mu^2}{2\lambda} = \frac{v^2}{2}$

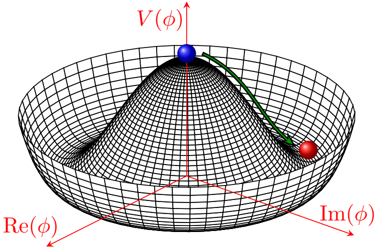

Higgs field expansion around its ground state:

$$\phi(x) = \frac{1}{\sqrt{2}} \begin{pmatrix} 0 \\ v + h(x) \end{pmatrix}$$, $h(x)$ = real scalar field

Injecting the expansion of $\phi(x)$ in $\mathcal{L}_{\text{Higgs}}$ predicts that:

$$m_W = \frac{gv}{2}, \quad m_Z = \frac{\sqrt{g'^2 + g^2}v}{2}, \quad m_\gamma = 0, \quad \frac{m_W}{m_Z} = \cos(\theta_W)$$

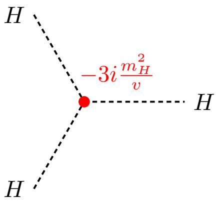

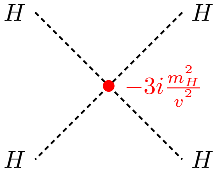

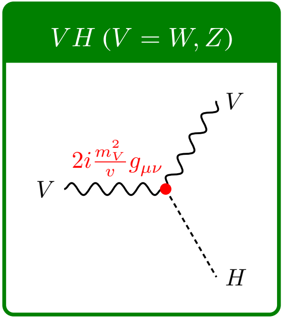

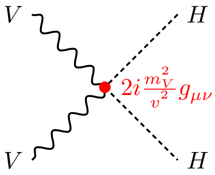

→ The BEH mechanism explains the mass of the bosons

NB: the Higgs mass (m_H) is a free parameter & is not predicted by the BEH mechanism

The BEH mechanism does not explain the mass of fermions

$\rightarrow$ Need for another mechanism

$$\mathcal{L}_{\text{Yukawa}} = -y_f(\bar{\psi}_L\phi\psi_R + \bar{\psi}_R\phi^\dagger\psi_L)$$

y_f = Yukawa coupling for the fermion f

After spontaneous symmetry breaking & expansion around the ground state:

$$m_f = -\frac{y_f v}{\sqrt{2}}$$

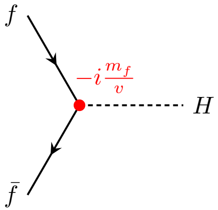

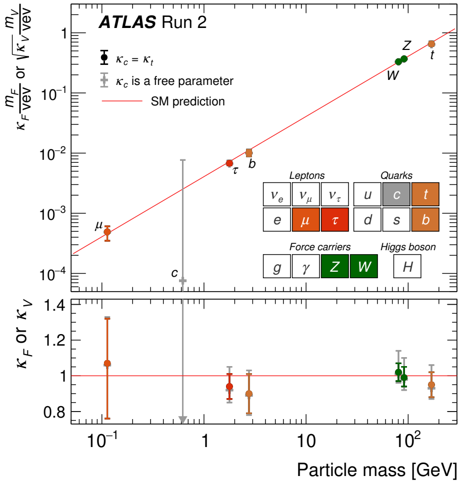

Since its discovery in 2012, many Higgs production modes (ggF, VBF, VH, $t\bar{t}H$)
& Higgs boson decays ($H \to \gamma\gamma, ZZ, W^+W^-, b\bar{b}, \tau^+\tau^-$)
predicted by the SM have been observed

Higgs sector might be a portal for open question of the SM and/or probing BSM theories
e.g. dark matter

Jets within ATLAS

Jet = hadronization of a parton (quark or gluon)
leading to a spray of collimated hadrons in the detector

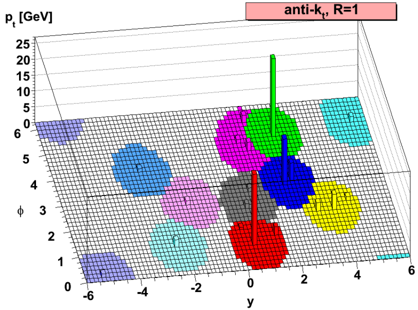

- **Reconstruction by clusterization of hits** in the detector approximately into cones of a certain angular distance (ΔR)

$$\Delta R_{ij} = \sqrt{(\eta_i - \eta_j)^2 + (\phi_i - \phi_j)^2}$$

$\rightarrow$ Jet $\approx$ "circle" in the η-ϕ plane

- Jets in ATLAS are reconstructed using **calorimeter and/or tracker based information**

- **Different types of jets**:
  - **Small-R jets**: $R = 0.4$
  - **Large-R jets**: $R = 1.0$
  - **Variable radius (VR) track jets**:

$$0.02 < R < 0.4$$
$$R = \frac{\rho}{p_{\mathrm{T}}}, \rho = 30 \text{ GeV}$$

Why different radius for jets?
$H \to b\bar{b}$ decay example

Low energy Higgs boson
$\to$ Resolved topology

High energy Higgs boson
$\to$ Boosted topology

Angular distance between jets

$$\Delta R \approx \frac{2m_H}{p_T^H}$$

$$m_H = 125 \text{ GeV}$$

$\Rightarrow$ boosted for
$p_T^H \approx$ few hundred of GeV

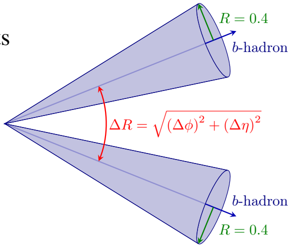

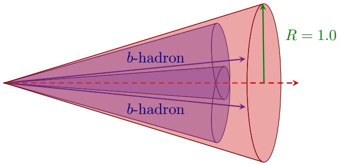

$pp \to Z(\to \nu\bar{\nu}) + H(\to b\bar{b})$ with 2 small-R jets

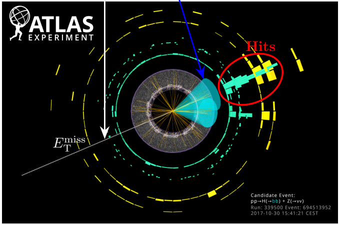

$pp \to W(\to \mu\nu) + H(\to b\bar{b})$ with a large-R jet

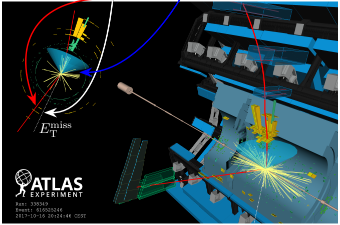

$\to$ Reconstruct the Higgs with 2 small-R or a large-R jet(s) depending on the regime

For the boosted topology, b-tagging criteria using the VR track-jets matched to the large-R jet

Small-R jets calibration procedure in ATLAS

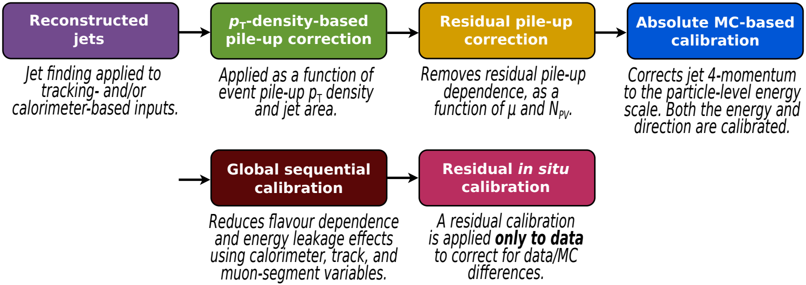

Several steps:

- **Reconstruction of jets**
- **Pile-up corrections**: remove biases due to pile-up
- **Absolute MC-based calibration**: correct reconstructed jet four-momentum to the particle-level energy + biases for the jet η reconstruction
- **Global Sequential Calibration**: corrections to reduce fluctuation effects
- **In-situ correction**: correct data for differences w.r.t simulation

Standard model

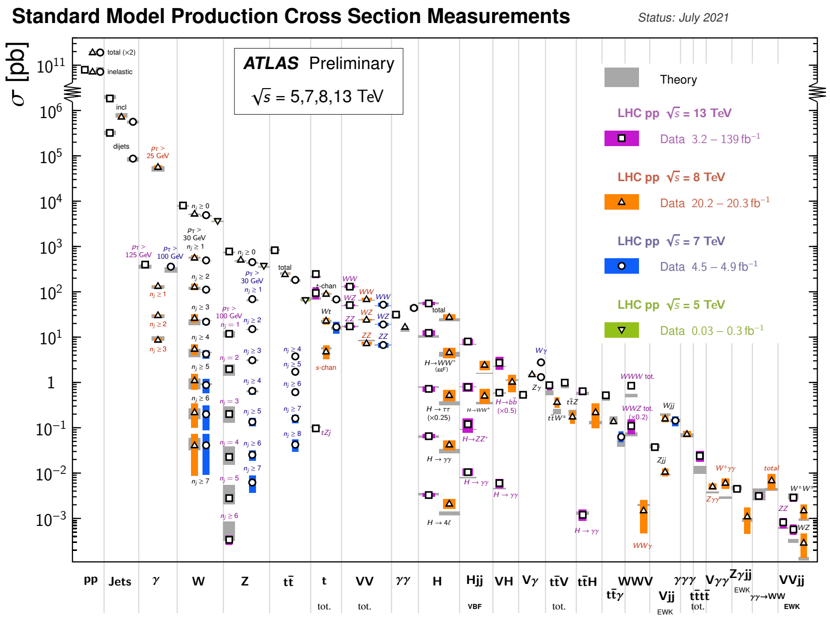
Standard Model Production Cross Section Measurements
Status: July 2021
ATLAS Preliminary
√s = 5,7,8,13 TeV
σ [pb]
Theory
LHC pp √s = 13 TeV
Data 3.2 – 139 fb⁻¹
LHC pp √s = 8 TeV
Data 20.2 – 20.3 fb⁻¹
LHC pp √s = 7 TeV
Data 4.5 – 4.9 fb⁻¹
LHC pp √s = 5 TeV
Data 0.03 – 0.3 fb⁻¹
pp
Jets
γ
W
Z
tt̄
t
VV
γγ
H
Hjj
VH
Vγ
tt̄V
tt̄H
tt̄γ
WWV
Vjj
γγγ
tt̄tt̄
Vγγ
Zγjj
γγ→WW
VVjj
tot.
VBF
EWK

Main Higgs production mode

ggF

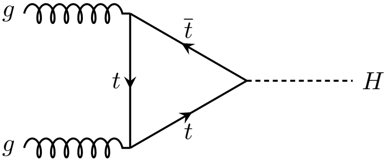

VBF

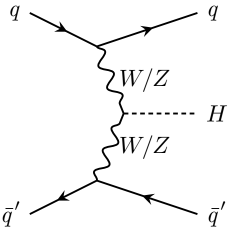

VH

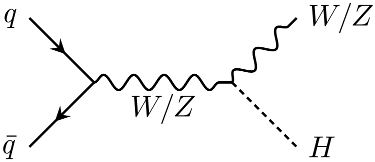

$t\bar{t}H$ or $b\bar{b}H$

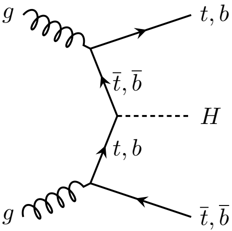

tH

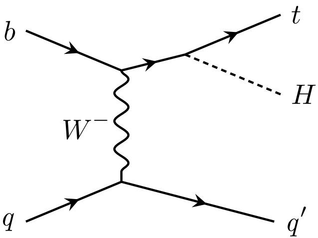

Higgs decay mode

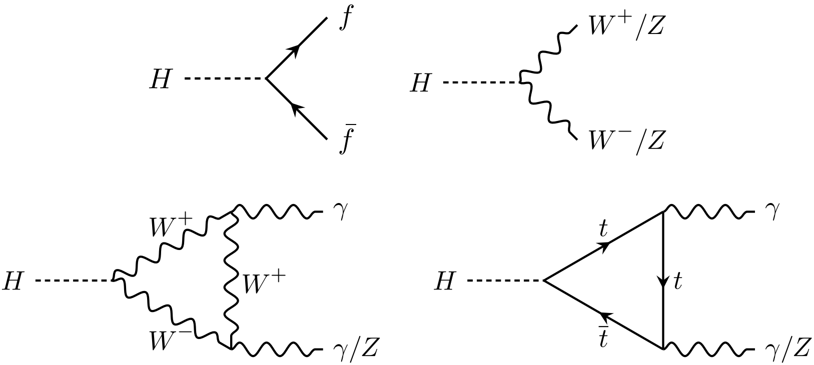

ATLAS measurement of production and decay modes

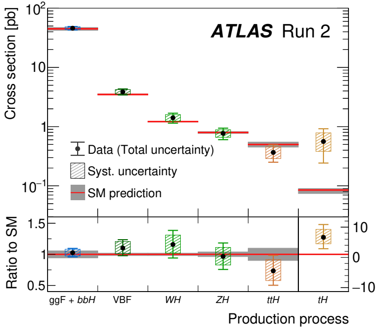

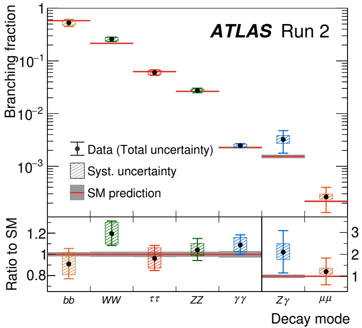

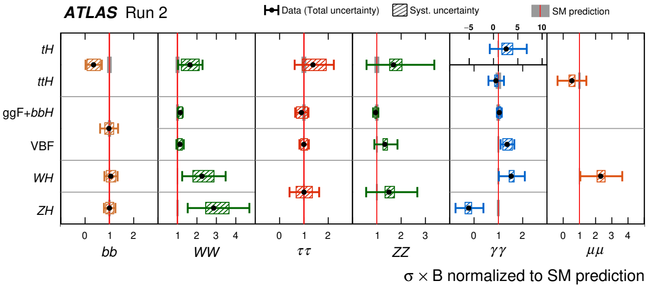

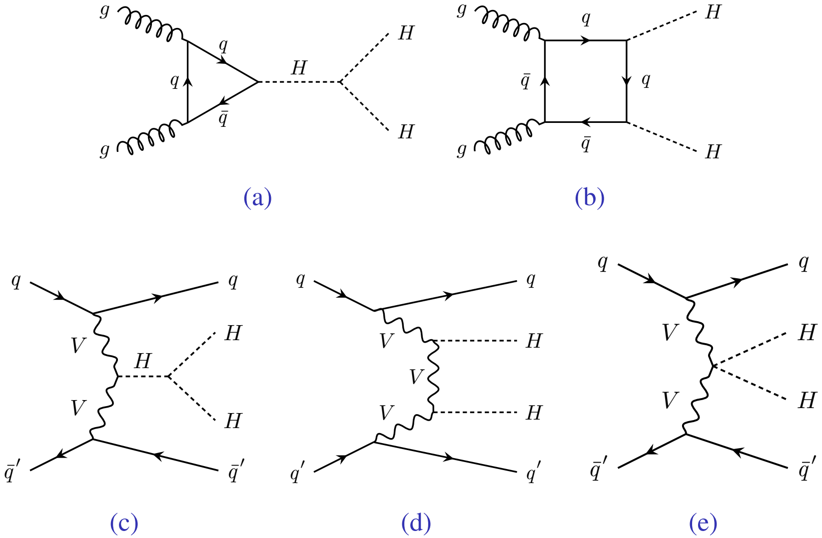

Feynman diagrams of the di-Higgs a and b gluon-gluon fusion, and c, d and e vector boson fusion production modes.

CKM matrix

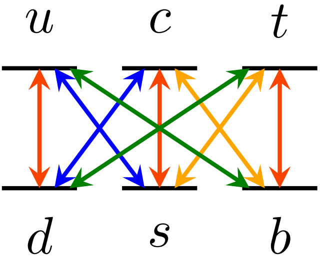

$|V_{qq'}| \approx 1$

$|V_{qq'}| \approx \lambda$

$|V_{qq'}| \approx \lambda^2$

$|V_{qq'}| \approx \lambda^3$

CKM = provides probability of a transition between two quarks when the mediator is a W boson
probability which is proportional to $|V_{qq'}|^2$
$\lambda \approx 0.226$

CMS

CMS $VH(b\bar{b})$, Run 2: $\mu_{VH}^{bb} = 1.15^{+0.22}_{-0.20}$

Phys. Rev. D 109 (2024) 092011

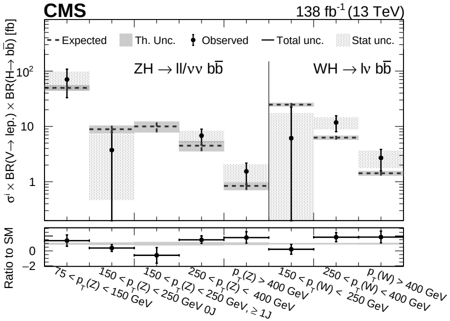

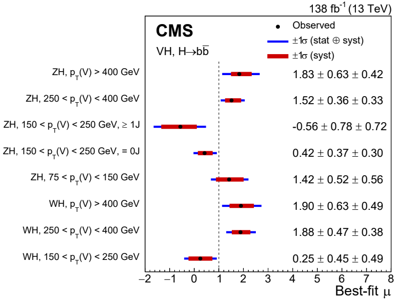

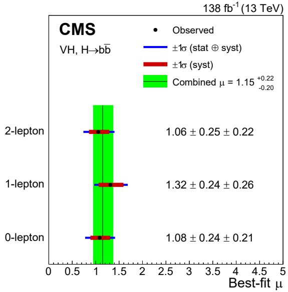

Phys. Rev. Lett. 131 (2023) 061801

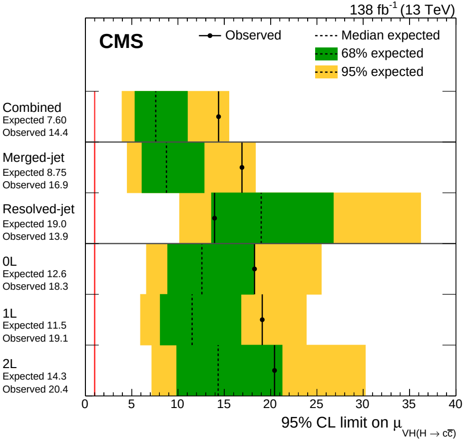

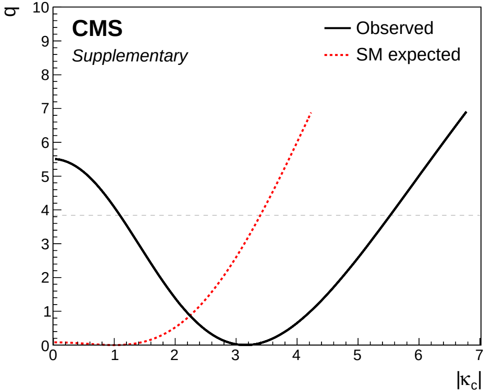

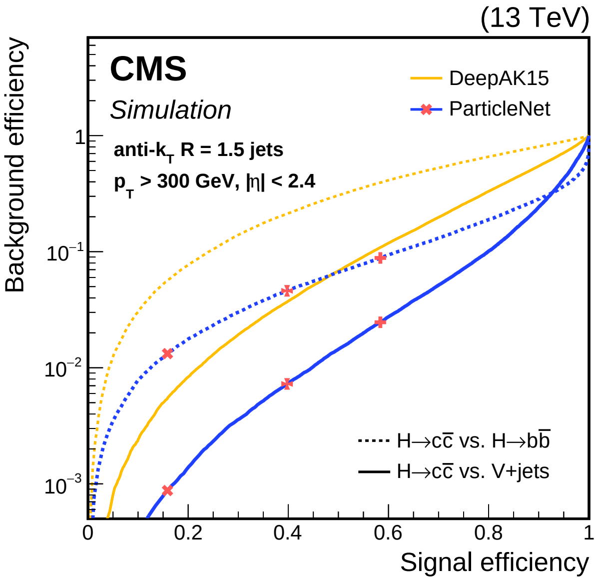
(13 TeV)
CMS
Simulation
anti-k_T R = 1.5 jets
p_T > 300 GeV, |η| < 2.4
DeepAK15
ParticleNet
H→cc̄ vs. H→bb̄
H→cc̄ vs. V+jets
Background efficiency
Signal efficiency
1
10^−1
10^−2
10^−3
0
0.2
0.4
0.6
0.8
1